Hydrocarbon ions in fuel-rich, CH_4–C_2H_2–O_2 flames as a probe for the initiation of soot: an experimental approach

SCOTT D. TANNER,[1] JOHN M. GOODINGS, AND DIETHARD K. BOHME
York University, Department of Chemistry, 4700 Keele Street, Downsview, Ont., Canada M3J 1P3

Received October 22, 1980

This paper was presented at a Special Symposium "The Structure and Thermochemistry of Gaseous Ions", held in honour of Dr. F. P. Lossing of the National Research Council of Canada, during the Second Canadian Conference on the Gas Phase Chemistry of Ions, Trent University, June 5–8, 1980, and is dedicated to him on the occasion of his 65th birthday

SCOTT D. TANNER, JOHN M. GOODINGS and DIETHARD K. BOHME. Can. J. Chem. **59**, 1760 (1981).

The natural hydrocarbon ions $C_nH_x^{\pm}$ ($n \geq 2$, $x \geq 0$) present in premixed, fuel-rich, nearly sooting, CH_4–C_2H_2–O_2 flames at atmospheric pressure were studied as a probe of the early chemical stages of soot formation. Ion concentration profiles were measured mass-spectrometrically along the flame axis through the reaction zone into the burnt gas downstream. Total ionization profiles were examined for their dependence on both temperature and equivalence ratio, ϕ. Families of individual $C_nH_x^-$ negative ion profiles exhibit concentration peaks in three distinct regions; predominantly oxygenated ions occur upstream, giving way to moderately unsaturated hydrocarbon ions near the end of the reaction zone, leading to highly unsaturated carbonaceous ions further downstream. The concentrations of the downstream ions alternate with the parity of n, the even-n species being larger. Series of $C_nH_x^+$ positive ion profiles, for a given n, show profile peak positions which move steadily downstream with decreasing x, indicative of progressive dehydrogenation. The positive ion chemistry of these series is essentially independent of n. As ϕ is increased at constant temperature towards the sooting point, the concentrations of $C_nH_x^{\pm}$ ions increase while those of the oxygenated ions decrease; the positive ions show a relative enhancement of species having high values of n.

SCOTT D. TANNER, JOHN M. GOODINGS et DIETHARD K. BOHME. Can. J. Chem. **59**, 1760 (1981).

Dans le but d'évaluer la nature des réactions impliquées dans les stades préliminaires de la formation de la suie, on a étudié les ions des hydrocarbures naturels, $C_nH_x^{\pm}$ ($n \geq 2$, $x \geq 0$), présents à la pression atmosphériques dans des flammes de CH_4–C_2H_2–O_2, riches en combustible, prémélangés et pratiquement au point de former de la suie. On a mesuré les profils des concentrations des ions par spectrométrie de masse en fonction de l'axe de la flamme traversant la zone de réaction et procédant vers la section des gaz brûlés. On a examiné les profils d'ionisation totale tant au point de vue de l'influence de la température que du point de vue du rapport d'équivalence, ϕ. Les familles individuelles d'ions négatifs $C_nH_x^-$ présentent des pics de concentrations dans trois régions distinctes; près de la zone de réaction, on retrouve principalement des ions oxygénés et si on procède vers la zone des gaz brulés on retrouve d'abord des ions d'hydrocarbures modérément insaturés puis des ions carbonés fortement insaturés. Les concentrations des ions dans la zone des gaz brulés alternent avec la parité de n; les concentrations des espèces où n est pair sont plus élevées. Les séries de profils des ions positifs $C_nH_x^+$, pour une valeur donnée de n, indiquent que le profil des positions du pic se déplace d'une façon régulière vers la zone des gaz brulés lorsque n diminue; ceci indique une déshydrogénation progressive. La chimie des ions positifs de ces séries est pratiquement indépendante de n. Lorsqu'augmente ϕ, à température constante, vers le point de formation de suie, les concentrations des ions $C_nH_x^{\pm}$ augmentent alors que celles des ions oxygénés diminuent et les concentrations des ions positifs sont relativement plus élevés lorsque les valeurs de n sont élevées.

[Traduit par le journal]

Introduction

Flame chemists are divided on the mechanism of soot formation in hydrocarbon combustion. There are proponents of both an ion-based synthesis of carbon and a neutral chemistry scheme. Most of the research which has been done on soot has been directed at its phenomenology in the burnt gas (1). This is too late in the flame to gain information about the initial chemistry of soot formation. One technique with which it is possible to study the reaction zone of a flame involves the measurement of ion concentrations and their axial profiles with a flame-ion mass spectrometer. An understanding of the relevant ion–molecule reactions then allows the flame-ion data to be interpreted to give insight into both the ionic and the neutral chemical evolution of the flame.

Detailed studies of the ionic composition of flames have very recently been reported for fuel-rich methane combustion by Goodings *et al.* (2, 3) and for fuel-rich and sooting acetylene and ethylene flames by Tse *et al.* (4) and Delfau *et al.* (5). In each of these works particular attention was drawn to the observation of high-mass carbonaceous ions in the burnt gas just downstream of the luminous flame front. Goodings *et al.* (2, 3) measured concentration profiles for all detectable ions of both polarities for $m/e < 100$ amu. The chemistry of their formation, interconversion, and loss was discussed. The observation of carbonaceous positive ions for $m/e < 200$ amu in the reaction zone of a

[1]Present address: Sciex Inc., 55 Glencameron Rd., #202, Thornhill, Ont., Canada L3T 1P2.

0008-4042/81/121760-11$01.00/0
©1981 National Research Council of Canada/Conseil national de recherches du Canada

fuel-rich acetylene flame was taken by Tse *et al.* (4) to indicate early pyrolysis of the fuel. The novel application of a 360° magnetic mass analyzer by Delfau *et al.* (5) permitted the observation of positive ions up to $m/e \simeq 7000$ amu downstream in sooting flames.

The present work was undertaken in order to provide some insight into the mechanisms of formation of these carbonaceous ions in the belief that they constitute a source of information about the early chemical stage of soot formation. The evolution of the flame-ion distribution was monitored through the reaction zones of a fuel-rich methane–oxygen flame and a nearly-sooting flame with acetylene added to the methane fuel. The excellent spatial resolution provided by the flame-ion mass spectrometer employed for these studies permitted the ion distribution of these flames to be mapped in detail. Additional measurements were made to record the response of this distribution when sooting conditions are approached.

The experimental results of this investigation and a preliminary discussion are presented in this paper. A considerable range of observations is organized in summary form at the end of the paper. The detailed interpretation of these data will be discussed in a later publication.

Experimental

The ion concentration data were obtained with a flame-ion mass spectrometer which has been described previously (2). A fuel-rich premixed, laminar flame was stabilized vertically on a simple, cylindrical, quartz burner at atmospheric pressure. The flame was conical with a base diameter of about 4 mm and a height of about 6 mm with a rounded tip. It was surrounded by a flowing argon shield to exclude atmospheric air. Compressed methane and oxygen of CP grade (>99% CH_4, >99.6% O_2) and acetylene of Purified grade (>99.6% C_2H_2 dissolved in acetone) were used directly from the cylinders without further purification.

Two flames were studied in detail in this work. One of these was a pure methane–oxygen flame having an equivalence ratio $\phi = 2.15$ (alternatively, a carbon/oxygen ratio C/O = 0.538). Ionic data for this flame have been reported previously (2, 3). A more fuel-rich methane flame with added acetylene having the same burnt-gas temperature as measured with a pneumatic probe (6) was also studied. The equivalence ratio for such a mixed-fuel flame of unburnt composition CH_4:C_2H_2:$O_2 = a:b:c$ is given by $\phi = (4a + 5b)/2c$ (C/O = $(a + 2b)/2c$). A more fuel-rich flame is cooler than another one nearer to stoichiometric composition, whereas C_2H_2–O_2 mixtures burn at higher temperatures than do CH_4–O_2 mixtures. Therefore, by properly choosing the CH_4–C_2H_2 fuel mixture, a fuel-rich flame may be burned having the same temperature as a less fuel-rich pure CH_4–O_2 flame. It was found that a flame having $\phi = 2.47$ (C/O = 0.696) and containing 17.7% C_2H_2 in the fuel had a temperature in the burnt gas at a distance $z = 3$ mm downstream of the reaction zone which was the same as that measured at the same point for the methane–oxygen flame with $\phi = 2.15$. The flames were of the same shape and size so that the distance scales upstream of, and within, the reaction zones were comparable. A faint yellow luminescence from soot particles was observed for the more fuel-rich flame.

The burner itself was mounted on a motor-driven carriage, and the flame axis was carefully aligned with respect to the mass spectrometer sampling orifice. A voltage proportional to the calibrated displacement of the burner carriage was fed to the X-axis of an XY recorder such that 0.1 mm along the flame axis corresponded to either 1.00 cm or 0.75 cm on the recorder. In a typical experiment, the quadrupole mass filter was tuned to a specific m/e and the output from an electrometer connected to a Faraday cage was coupled to the Y-axis of the XY recorder. In this manner, the concentration profile of the ion species corresponding to the specified m/e was recorded as a function of distance axially through the tip of the flame. Total ionization profiles were obtained in the same fashion by removing the dc voltage from the mass filter. The pressure in the second vacuum chamber of the mass spectrometer was monitored with an ionization gauge and displayed on a second XY recorder. The pressure profile derived in this manner showed a minimum corresponding to the downstream edge of the reaction zone. This minimum was adopted as a reproducible origin ($z = 0$ mm) *in the flame* for the distance scale of the ion profiles.

In the experiments reported previously from this laboratory, the flame ions were sampled through a pinhole 0.1 mm in diameter in a platinum–iridium disc welded into a water-cooled stainless-steel mounting. The flat disc against which the flame burned was approximately 2.0 mm in diameter. For the present experiments, this sampling nozzle was replaced with a thin-walled chromium cone which had a sharp-edged orifice of diameter 0.10 mm at its apex and a total tip diameter of approximately 0.28 mm. This sampling cone was made in a manner similar to that suggested by Burdett and Hayhurst (7). The change in orifice design considerably decreased the thickness of the thermal/momentum boundary layer which covers the sampling plate as discussed in the work of Hayhurst and co-workers (8, 9). It is known that the gas sample may be chemically perturbed during passage through the boundary layer. One reaction which proceeds in this region is the three-body hydration of H_3O^+ (9). In the present study, the ratio $R = [H_3O^+ \cdot H_2O]/[H_3O^+]$ was observed to decrease from a value of $R = 0.34$ obtained with the "old" Pt/Ir sampling disc to $R = 0.09$ with the Cr nozzle. This may be taken as evidence of a considerable decrease in the thickness of the boundary layer. An additional advantage of using the sharp-tipped Cr nozzle over the blunt Pt/Ir disc is an increased spatial resolution. This may be understood by making reference to the flow streamline calculations of Hayhurst *et al.* (8) for a conical nozzle similar to that employed in the present study. The tip of this Cr nozzle is blunt over a radius which is less than the stagnation radius. The Pt/Ir disc, on the other hand, is considerably more blunt causing a thicker momentum boundary layer; this, in turn, causes an increase in the stagnation radius. As a result, some of the ions included in the sample drawn through the Pt/Ir nozzle are taken from a region further from the flame axis than are included in the sample passing through the Cr nozzle. When sampling upstream in a conical flame, gas originating at a point further from the flame axis can derive from a region in the flame downstream of the sampling point, thereby decreasing the spatial resolution.

Differences between the ion profiles presented here and those reported earlier for the same $\phi = 2.15$ flame (2, 3) may be ascribed to these changes in sampling conditions. In fact, the maximum total positive ion signal detected with the two different sampling nozzles was the same within experimental error, although the maximum negative ion signal decreased by a

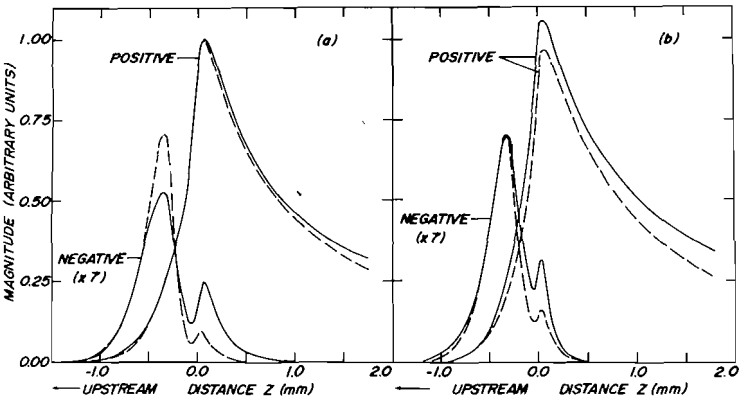

FIG. 1. Total positive and negative ionization profiles: (*a*) for two flames having similar adiabatic flame temperatures, T_{ad} but different equivalence ratios, ϕ. Dashed curves: $\phi = 2.15$ (C/O = 0.538), no C_2H_2, $T_{ad} = 2455$ K. Solid curves: $\phi = 2.47$ (C/O = 0.696), 17.7% C_2H_2, $T_{ad} = 2443$ K. % C_2H_2 refers to the percentage in the fuel; (*b*) for two CH_4–C_2H_2–O_2 flames having similar ϕ's but different values of T_{ad}. Dashed curves: $\phi = 2.22$ (C/O = 0.560), 1.1% C_2H_2, $T_{ad} = 2401$ K. Solid curves: $\phi = 2.23$ (C/O = 0.587), 7.1% C_2H_2, $T_{ad} = 2488$ K.

factor of 3.5 when the Cr nozzle was used (c.f. Fig. 1(*a*) here with Fig. 1(*b*) of ref. 3). This latter decrease is expected because the boundary layer cooling is reduced when sampling with the new nozzle. Consequently, negative ion equilibria shift in the endothermic direction causing electron detachment from negative ions; the free electron concentration is enhanced at the expense of the negative ion concentration. It should be clearly understood, however, that all of the data considered hereafter, including those for the $\phi = 2.15$ flame, were obtained using the new Cr sampling nozzle.

A quadrupole mass filter discriminates to some extent against the transmission of larger *m/e* ions. The effect is more pronounced when the resolving power of the filter is increased. For most of the experiments reported here, a relatively high resolving power was employed in order to distinguish between neighbouring ions of high *m/e*. For this reason, care was taken to assure that the resolving power was maintained constant for all the experiments involving relative magnitudes. In this way, the mass discrimination profile was maintained constant, and trends in the relative magnitudes of ion signals at the same mass numbers in different flames are still valid. In a few instances, the resolving power was lowered either to gain an appreciation for the extent of the mass discrimination or to increase the sensitivity for the larger *m/e* ions.

In order to achieve a consistent set of ion signals, a reference ion profile was recorded frequently during the experiments. The magnitude of each profile was normalized to the maximum signal measured for the total ionization profile of the same polarity. These normalized ion signal magnitudes (all < 1.0) are referred to as *relative magnitudes*, although those for positive ions have been multiplied by 10^4 and those for negative ions by 10^3 to eliminate cumbersome negative powers of ten. Magnitude ratios for individual ion profiles for different flames may be obtained by using the ratio of the peak magnitudes of the total ionization profiles as a multiplier applied to the relative magnitudes. The relevant peak magnitudes are given in Fig. 1.

Results and Preliminary Discussion

Total Ionization Profiles

Total ionization profiles for the two flames which were studied in detail in this work are given in Fig. 1(*a*). The phenomenology of the profiles for the flame having $\phi = 2.15$ (C/O = 0.538) has been discussed previously (3); the improved spatial resolution is apparent in the negative ionization profile whose minimum between the two peaks earlier had been hidden when sampling with the Pt/Ir nozzle. The profiles may be contrasted with those given in Fig. 1(*b*) for two flames which have similar equivalence ratios but distinctly different adiabatic flame temperatures.

Several observations can be made from these results. The first is that the peak magnitude of the total positive ionization curve increases with increasing flame temperature. Such a trend is consistent with an increase in the rate of chemi-ionization with temperature.

Secondly, the magnitude of the upstream peak of the negative ionization profile seems to depend mainly on the equivalence ratio of the unburnt gas. Several reasons for this dependence may be envisaged. The decrease with increasing ϕ (or C/O ratio) may result from a decreased rate of attachment of electrons as would result, for example, from a decrease in the concentration of O_2. Alternatively, the rate of loss of negative ions may be enhanced by an increase in the non-equilibrium concentration of radicals, especially H, which participate in ion–radical associative detachment reactions.

Finally, the magnitude of the downstream maximum of the total negative ionization profile is seen to increase considerably with an increase in both ϕ (or C/O ratio) and the flame temperature. This behaviour is consistent with an increase in the rate of electron attachment to hydrocarbon neutrals, for example polyacetylenes or their radicals, whose

concentrations increase rapidly with both equivalence ratio and temperature.

Downstream Ion Spectra

A more detailed view of the ionic composition of the flame is provided by measurements of the ion mass spectra. Figure 2 presents the spectra measured at a distance $z = 0.05 \pm 0.02$ mm downstream of the reaction zone of the flame with $\phi = 2.47$. At this point in the flame the total positive and negative ionization profiles maximize. It should be noted that the sampling position is referenced to an origin within the flame itself. Such a procedure is necessary given the high spatial resolution of this method. Our experience has shown that the observed mass spectra can be extremely sensitive to small changes in the sampling position within, and downstream of, the reaction zone.

Negative Ions: It is significant that the dominant negative ions in this fuel-rich flame are the highly unsaturated hydrocarbons $C_nH_x^-$ with $n \geq 2$ and $x \leq 5$. Operation of the mass filter at low resolving power permitted the detection of groups of ions spaced by roughly 12 amu having values of n up to and including 10. These are shown in Fig. 2(*a*) which, for the most part, gives the mass numbers of the maximum signals for the various ion groups. The individual ions which compose these broad groups were resolved at high resolving power, as shown in Fig. 2(*b*). It was noticed that the ions corresponding to C_2H^- and C_4H^- have significantly higher concentrations than do the ions with odd values of n. In fact, this alternation of intensity with the parity of n was observed all the way up to $n \sim 10$ in the experiments with low resolving power, and is consistent with the earlier observations reported by Green (10). This alternation attests to the importance of polyacetylenes or their radicals at this point in the flame. Nearly all of the hydrocarbon ions are more abundant in the more fuel-rich flame.

Positive Ions: The groups of $C_nH_x^+$ ions observed in the positive ion spectrum shown in Fig. 2(*c*) are remarkable for their similarity to one another in structure. The lower-x, more unsaturated components of each family seem to be strongly preferred; the largest signal in each family occurs for $x = 3$. Since the spectra for the different families are similar, it would seem that the chemistry of the $C_nH_x^+$ ions is essentially independent of n. The fall-off in the magnitudes of the $C_nH_x^+$ ion groups with increasing n may reflect to some extent an increase in mass discrimination of the quadrupole mass filter with increasing mass number at the high resolving power used to obtain these data. Consequently, this overall trend in the magnitudes of the $C_nH_x^+$ ion signals with n is not included in the summary of results given at the end of the paper. A comparison with the spectrum obtained at the same position in the more fuel-lean ($\phi = 2.15$, no C_2H_2) flame (not shown) revealed several other noteworthy features (11). Ions corresponding to $n \leq 2$ and oxygenated species have higher concentrations in the flame with $\phi = 2.15$, whereas ions corresponding to $n > 2$ seem to be more abundant in the more fuel-rich flame. The degree of this enhancement increases with increasing n. Furthermore, within a group of given n, there is a relative enhancement of ions with small x.

Reaction Zone

A view of the evolution of the ionic composition requires measurements of the axial concentration profiles for the individual ion species. In this section we present profiles measured with the intent to characterize their early behaviour upstream in the reaction zone.

Positive Ions: Figure 3 shows normalized profiles measured for the $C_4H_x^+$ family of ions from 49 to 57 amu. There is a clearly-resolved progression downstream from high to low mass ions. This behaviour is exemplary of that observed for the other $C_nH_x^+$ families.

More than 70 individual positive ion concentration profiles were measured for each flame studied. This vast amount of detailed information is unwieldy to manipulate. The data for the flame with $\phi = 2.47$ are presented in Fig. 4 in such a manner as to provide a simplified overview. The mass of each ion is plotted against the position (distance coordinate, z) at which the corresponding profile was observed to maximize. We have called such a plot a profile–peak–position or 3P plot. It provides an appreciation for the spatial relationships of the various ion concentration maxima at a glance. Similar data for the $\phi = 2.15$ flame are available (11). Of course, the details of the shapes of the profiles are necessarily lost in such a treatment. In addition to the profile peaks noted in Fig. 4, several profiles displayed broad peaks with maxima well downstream, given in Table 1. These involve the protonation of major combustion products in the burnt gas (H_2O, CO, CO_2 and their isotopic derivatives; a small amount of nitrogen is present from air entrainment, which leads to NH_3).

In the interpretation of this 3P plot it should be remembered that the precise locations and magnitudes of the profile maxima are intimately related to

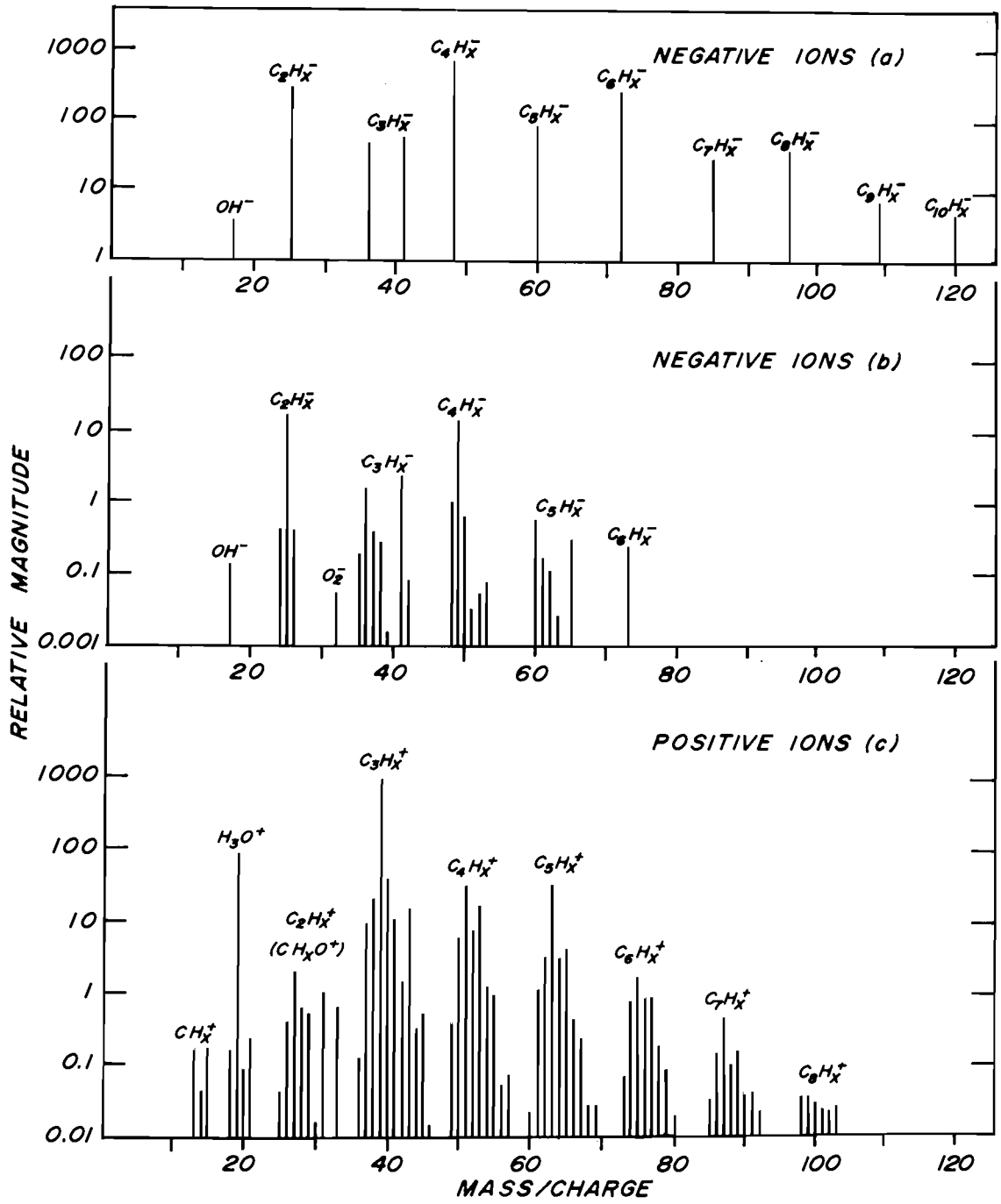

FIG. 2. Ion mass spectra recorded at a distance $z = 0.04 \pm 0.02$ mm downstream of the reaction zone of a CH_4–C_2H_2–O_2 flame (ϕ = 2.47, 17.7% C_2H_2). (*a*) Negative ions, low resolving power. (*b*) Negative ions, high resolving power. (*c*) Positive ions, high resolving power.

the rates of the formation and loss processes of the ions concerned. A large relative magnitude in the peak concentration of an ion may indicate either a relatively lower reactivity of the ion or a more prolific source.

Figure 4 shows eight distinct series of concentration maxima. The members of each series shift monotonically downstream with decreasing amu. Each series originates well upstream near the beginning of the reaction zone with its highest amu

TABLE 1. Peak positions of positive ion concentration profiles which showed broad maxima downstream of $z = 0.4$ mm

amu	Assignment	Peak position[a]	Relative magnitude
18	H_2O^+ (NH_4^+)	>3.3	>3.1
19	H_3O^+	2.68±0.08	384
20	H_2DO^+	2.60±0.10	0.31
21	$H_3{}^{18}O^+$	2.70±0.08	0.82
29	CHO^+	2.59±0.09	0.80
37	$H_3O^+ \cdot H_2O$	2.93±0.09	20.5
45	CHO_2^+	0.72±0.08	0.70
46	$^{13}CHO_2^+$, CDO_2^+, $CH^{17}O^{16}O^+$	0.68±0.09	0.02

[a]Measured in mm with respect to the origin ($z = 0$) at the end of the reaction zone.

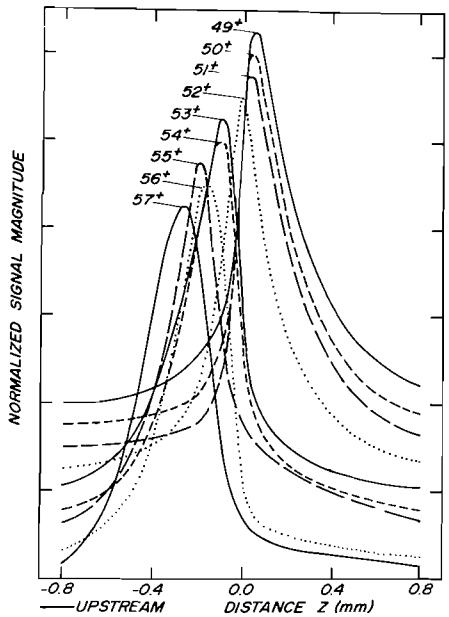

FIG. 3. Positive ion profiles observed for the ions from 49 to 57 amu. The magnitudes of the profiles have been normalized, and the zero baseline has been displaced vertically by a 1/4 scale interval per amu. These data were obtained for the flame with $\phi = 2.22$, 1.1% C_2H_2, $T_{ad} = 2401$ K.

members, and ends downstream at about $z = 0.1$ mm where its lowest amu members are gathered. The series are separated from each other by approximately 12 amu.

The relative magnitudes of the peak concentrations alternate quite regularly within each series, with those for ions of odd amu being appreciably larger than those for even amu ions. Over the limited mass range of any one of the eight series, mass discrimination effects are not significant. On the other hand, mass discrimination may play a significant role in the apparent decay in the relative magnitudes observed for the eight series, particularly beyond about 60 amu, at the high resolving power employed for these measurements. Therefore, this latter trend is not included in the summary of results given at the end of the paper. The actual concentrations of the higher mass ions may be quite considerable and comparable to the concentrations of the lower mass ions.

With the exception of a number of ions which may constitute sub-series of empirical formulae $C_nH_xO^+$ corresponding, for example, to protonated alcohols and aldehydes, the majority of the detected ions appear to be of the type $C_nH_x^+$ with n taking the values 1 through 8 and x taking values in the range 0 to $(2n + 3)$. Each value of n denotes a separate series for which the peak positions of the individual members are determined by the value of x. The spatial evolution of each series reflects a stepwise dehydrogenation leading to the highly unsaturated carbonaceous products at the end of the reaction zone. Presumably the higher-n homologues of these series ($n > 8$) are also present, but these were beyond the range of detection.

Negative Ions: The negative ion 3P plot for the flame with $\phi = 2.47$ is given in Fig. 5. It shows rather less structure than that for the positive ions and provides less insight into the assignment of the corresponding ion identities. Nearly all of the negative ion profiles show a maximum well upstream near the beginning of the reaction zone. All of these subsequently show a rather abrupt decrease with many recovering to a secondary maximum just downstream of the reaction zone. Some of these profiles show one additional maximum in the "valley" of the total ionization profile.

The larger of the upstream negative ion peaks are likely to be associated with oxygenated ions such as CHO_2^- and $C_2H_5O^-$ (45 amu), O_2^- (32 amu), $CHCO^-$ (41 amu), CO_3^- (60 amu), HCO_3^- (61 amu), and CH_2CHO^- (43 amu). One exception is the ion at 25 amu corresponding to C_2H^-.

The major downstream ions are readily identified as very highly unsaturated hydrocarbons. The most abundant of these are the acetylenic species

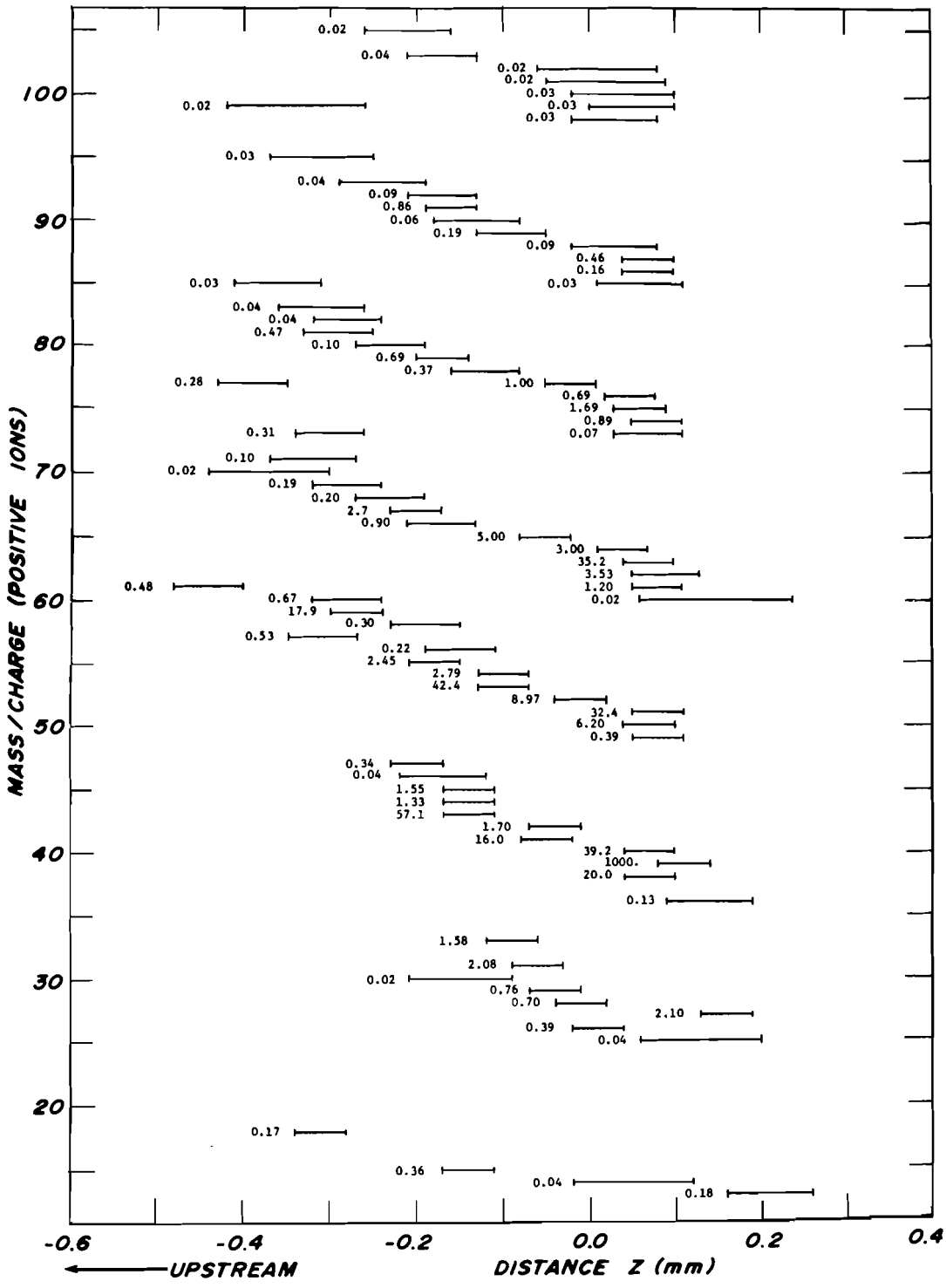

FIG. 4. The positive ion profile–peak–position (3P) plot for the flame with $\phi = 2.47$, 17.7% C_2H_2, $T_{ad} = 2443$ K. The number beside each bar is the relative magnitude of the profile maximum. The lengths of the bars represent the estimated uncertainties in the positions of the profiles which may arise from either the shapes or the magnitudes of the profiles.

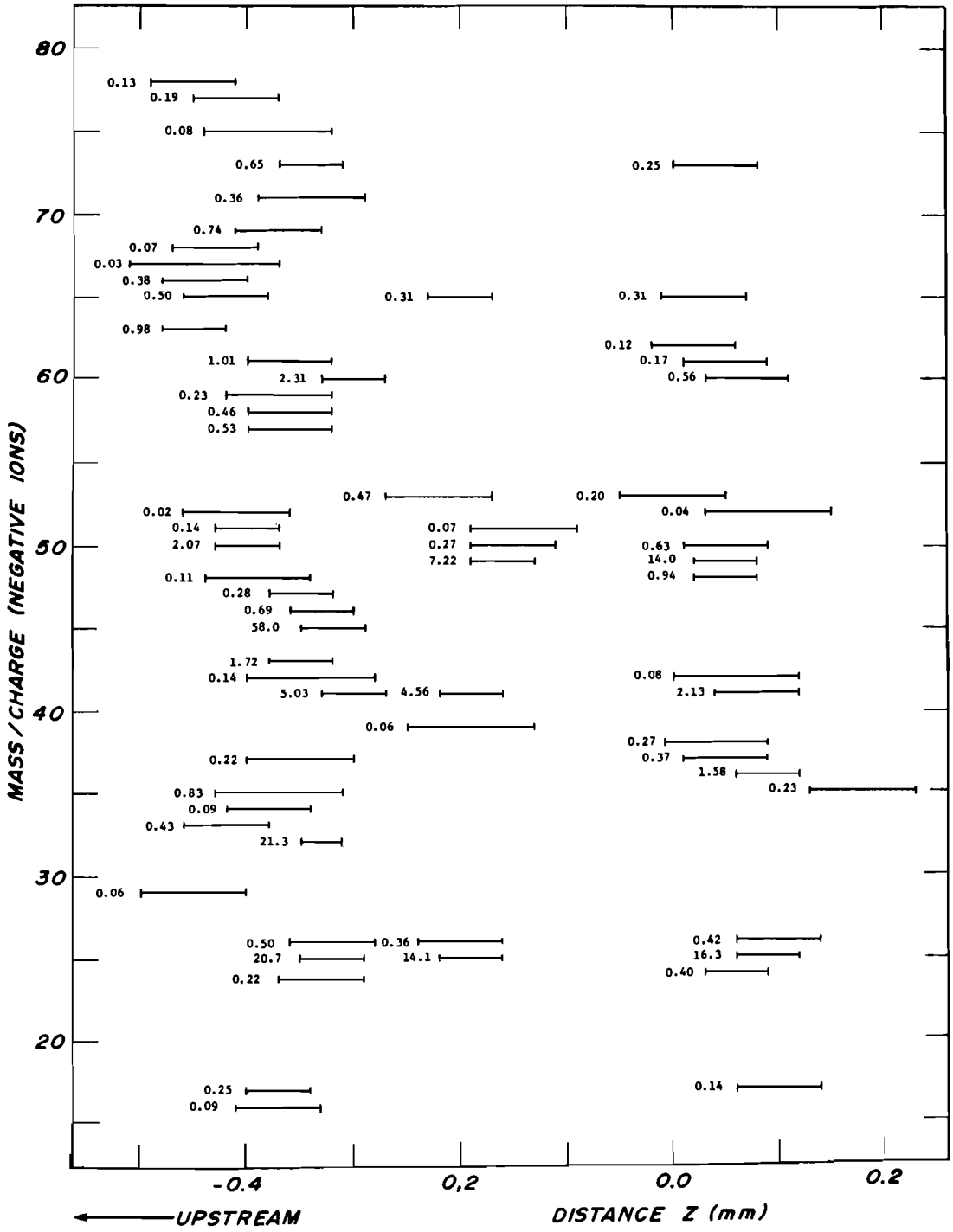

FIG. 5. The negative ion profile–peak–position (3P) plot for the flame with $\phi = 2.47$, 17.7% C_2H_2, $T_{ad} = 2443$ K. The number beside each bar is the relative magnitude of the profile maximum. The lengths of the bars represent the estimated uncertainties in the position of the profiles which may arise from either the shapes or the magnitudes of the profiles.

C_2H^- (25 amu) and C_4H^- (49 amu) with some C_6H^- (73 amu). The downstream odd-number carbon ion signals appear largest for $x = 0$ and 5; i.e., for C_3^- (36 amu), $C_3H_5^-$ (41 amu), and C_5^- (60 amu), $C_5H_5^-$ (65 amu).

The species C_2H^- and C_4H^- also show strong peaks in the intermediate valley region (as do their ^{13}C isotopic counterparts at 26 and 50 amu). The ion at 41 amu, which has been assigned as $CHCO^-$ upstream and as $C_3H_5^-$ downstream, also shows a major peak in this region. The remaining ions in the valley show much smaller maxima; interpreted as $C_nH_x^-$, these ions may represent moderately unsaturated intermediates in the overall dehydrogenation which appears to proceed through the reaction zone.

Variations with Fuel Composition

A comparison of the 3P plots for the flame having $\phi = 2.47$ (Figs. 4 and 5) with those for the flame having $\phi = 2.15$ (not shown) exhibited some interesting variations in both peak positions and magnitudes, albeit the gross features were quite insensitive to the change in equivalence ratio (11). As regards changes in peak positions, it was noticed that the upstream ion peak positions shifted downstream while the downstream ion peak positions shifted upstream with the change to the more fuel-lean flame. These features may reflect a real change in the width of the reaction zone resulting from changes in the reaction rates and burning velocity, and a change in the flame geometry. For the most part, however, these changes were only of the order of 0.05 mm. In general the peak magnitudes changed by not more than a factor of 5, although for a few ions changes as large as a factor of 20 were observed.

Of course, for a full appreciation of changes due to a change in fuel composition, there is no substitute for the profiles themselves. For example, the 3P plots do not contain information about the actual shapes of the peaks which reflect rates of formation and loss. Most of the observed peaks are skewed: the upstream peaks upstream and the downstream peaks downstream.

Some of the differences in shapes as well as peak magnitudes and positions observed with the change in fuel composition are illustrated in Figs. 6, 7, and 8 for several positive and negative ion profiles. It can be readily seen that the shapes in fact do not change dramatically over the range of conditions adopted in this study. This attests to the usefulness of the 3P-plot treatment introduced earlier.

As a general observation, the peak magnitudes of ions upstream decrease whereas the downstream peak magnitudes increase. This is illustrated for positive ions in Fig. 6. The increase downstream in the ions at mass 49 amu (C_4H^+) and 61 amu (C_5H^+) would appear to be associated with the increase in the acetylene concentration. The reason for the decrease in the upstream profile at 61 amu is less clear. A likely cause is proton transfer from protonated acetic acid to acetone present as an impurity in the added acetylene. The dramatic decrease in the intermediate CH_3^+ peak at 15 amu no doubt is due to its rapid reaction with C_2H_2 yielding $C_3H_3^+$ (12). A corresponding result is recorded for negative ions in Fig. 7. Here the downstream profiles at 25 and 60 amu (C_2H^- and C_5^-) increase with the addition of acetylene to the fuel. Of the upstream ions, C_2H^- increases at the expense of OH^- (and O^-, not shown) which is known to react with acetylene (13). The decrease in the upstream portion of the profile at 60 amu (CO_3^-) is likely a result of the depletion of its source ion, O^-.

As regards the individual ion profiles, only a few showed shifts in peak positions which were significantly larger than the small shifts of ± 0.05 mm discussed earlier. Notable amongst these are the profiles for H_3O^+, its hydrate $H_3O^+ \cdot H_2O$ and HCO^+. The last of these is shown in Fig. 8, where its peak is seen to shift by 1.79 ± 0.18 mm. The sharp peak upstream which does not show a shift may be identified as $C_2H_5^+$. The late downstream rise of HCO^+ may be related to the unusual persistence of $C_3H_3^+$. These two ions are believed to be coupled through the reaction (14)

$$C_3H_3^+ + O \rightleftharpoons HCO^+ + C_2H_2$$

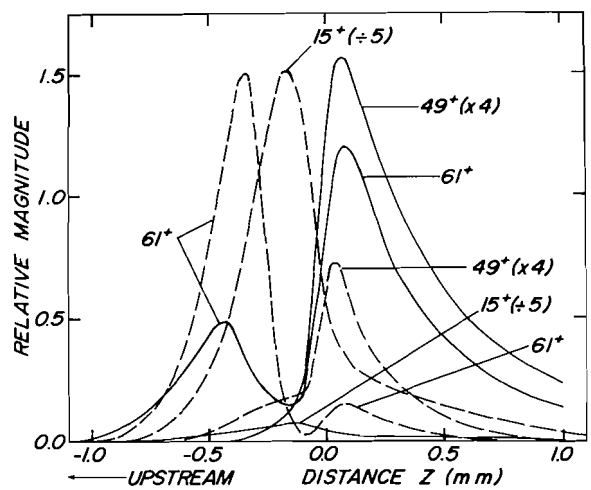

FIG. 6. A comparison of selected positive ion profiles which show significant changes in peak magnitudes measured for the flames having $\phi = 2.47$ (solid curves) and $\phi = 2.15$ (dashed curves).

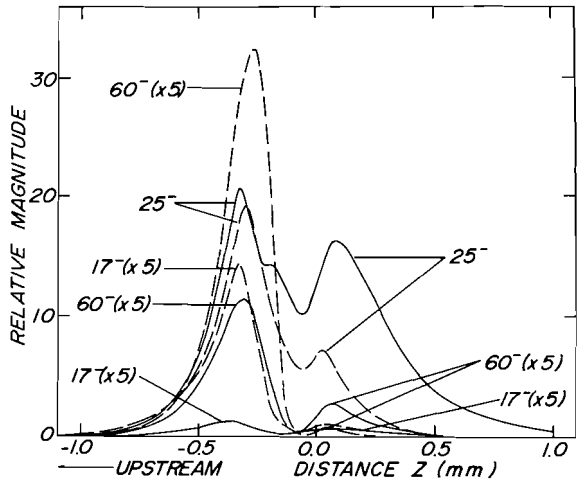

FIG. 7. A comparison of selected negative ion profiles which show significant changes in peak magnitudes measured for the flames having $\phi = 2.47$ (solid curves) and $\phi = 2.15$ (dashed curves). It should be noted that the peak magnitudes have been normalized to the maximum signal measured for the total negative ionization profile (see Fig. 1(*a*)).

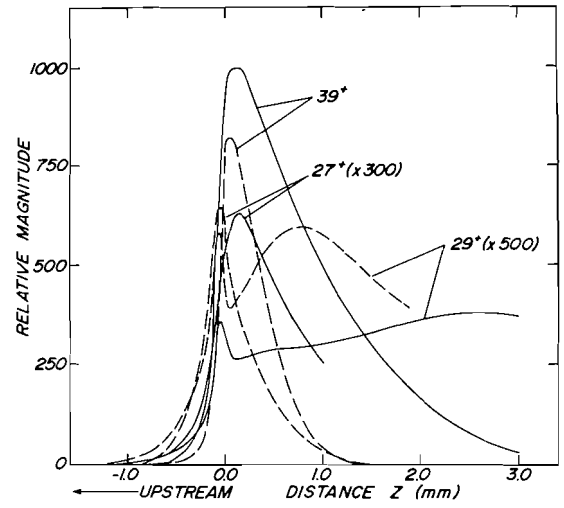

FIG. 8. A comparison of selected positive ion profiles which show significant changes in peak positions measured for the flames having $\phi = 2.47$ (solid curves) and $\phi = 2.15$ (dashed curves).

whose reverse rate will be enhanced by the added acetylene. Finally, the $C_2H_3^+$ profile at 27 amu shows the transition from a symmetric profile typical of intermediate ions to a more skewed profile characteristic of the more persistent ions downstream of the reaction zone. The small concomitant shift reflects the continued protonation of acetylene.

Summary

A large amount of experimental data has been presented in this report employing improved methods for the measurement of the flame-ion concentration profiles with high spatial resolution and novel approaches for their analysis. The following list summarizes many of the observations made in this study.

1. The spatial resolution of ion profile data is increased by the use of a conical sampling nozzle compared with a nozzle of more blunt geometry, for the same-sized orifice.

2. The peak magnitude of the total positive ionization curve increases with an increase in temperature; chemi-ionization has a positive temperature dependence (T-dependence).

3. The total negative ion profile is double-peaked. For fuel-rich flames, the magnitude of the upstream peak decreases with increasing equivalence ratio (negative ϕ-dependence) and has little T-dependence. The magnitude of the downstream peak shows both positive ϕ- and T-dependence.

4. The negative ion profile peaks for $C_nH_x^-$ ions appear in three distinct regions. (*i*) Oxygenated anions are found upstream; C_2H^- is an exception. (*ii*) Very highly unsaturated hydrocarbon ions are observed downstream peaking just beyond the reaction zone. Their concentrations alternate with the parity of n, the even-n species being larger. This implicates acetylene or its polymers in the anionic chemistry. For even n, the most abundant carbonaceous species are the acetylenic anions C_2H^-, C_4H^-, C_6H^-, ... with $x = 1$. For n odd, the most abundant tend to be those with $x = 0$ and 5. (*iii*) Moderately unsaturated hydrocarbon ions seem to be present in the intermediate region.

5. The positive ion peaks are observed to form a number of series through the flame reaction zone. (*i*) Each series is defined by the value of n, and the profile peak positions evolve downstream through the flame front with decreasing values of x, amounting to progressive dehydrogenation. (*ii*) The peak magnitudes tend to be larger for small values of x; the largest signal in each series is obtained for $x = 3$. Within each series, there is a fairly regular alternation in magnitude with x; the larger peaks are associated with odd values of x. (*iii*) The positive ion chemistry of these series seems to be essentially independent of the value of n.

6. As ϕ of a fuel-rich flame is increased at constant temperature towards the sooting point by the addition of acetylene, a number of changes occur. (*i*) The concentrations of the unsaturated positive and negative hydrocarbon ions within and

downstream of the reaction zone increase; the upstream (oxygenated) ions decrease. (*ii*) The profile peaks due to hydrocarbon ions spread out somewhat both upstream and downstream; possibly the thickness of the reaction zone is increased. (*iii*) The shapes of these profiles do not change greatly, except that they become more skewed in the downstream direction; a key factor to be considered is chemical reactions involving acetylene. (*iv*) The concentrations of positive ions having high n-values are enhanced relative to those of low n; the degree of this enhancement appears to increase with increasing n. Also, within a series of given n, there is a relative enhancement of ions with small x.

Acknowledgements

One of us (S.D.T.) is grateful for the award of an Ontario Graduate Scholarship. Support of this work by the Natural Sciences and Engineering Research Council of Canada under Grant Numbers A1604 (J.M.G.) and A6258 (D.K.B.) is acknowledged.

1. J. LAHAYE and G. PRADO. Chem. Phys. Carbon, **14**, 167 (1978).
2. J. M. GOODINGS, D. K. BOHME, and C.-W. NG. Combust. Flame, **36**, 27 (1979).
3. J. M. GOODINGS, D. K. BOHME, and C.-W. NG. Combust. Flame, **36**, 45 (1979).
4. R. S. TSE, P. MICHAUD, and J.-L. DELFAU. Nature, **272**, 153 (1978).
5. J.-L. DELFAU, P. MICHAUD, and A. BARASSIN. Combust. Sci. Technol. **20**, 165 (1979).
6. C.-W. NG. M.Sc. Thesis. York University, Downsview, Ont., Canada M3J 1P3. 1977.
7. N. A. BURDETT and A. N. HAYHURST. Proc. R. Soc. London A, **355**, 377 (1977).
8. A. N. HAYHURST, D. B. KITTELSON, and N. R. TELFORD. Combust. Flame, **28**, 123 (1977).
9. A. N. HAYHURST and D. B. KITTELSON. Combust. Flame, **28**, 137 (1977).
10. J. A. GREEN. 26th AGARD Propulsion and Energetics Panel, Pisa, Italy, AGARD Conference Proceedings No. 8. Vol. I. *Edited by* H. D. Wilsted. 1965. p. 191.
11. S. D. TANNER. Ph.D. Thesis, York University, Downsview, Ont., Canada M3J 1P3. 1980.
12. W. T. HUNTRESS, JR. Astrophys. J. Suppl. Ser. **33**, 495 (1977).
13. D. K. BOHME, G. I. MACKAY, H. I. SCHIFF, and R. S. HEMSWORTH. J. Chem. Phys. **61**, 2175 (1974).
14. J. M. GOODINGS, D. K. BOHME, and T. M. SUGDEN. Sixteenth Symposium (International) on Combustion, The Combustion Institute, Pittsburgh, PA. 1977. p. 891.